Control of beam halo formation through nonlinear damping and collimation

Kiran G. Sonnad and John R. Cary

Center for Integrated Plasma Studies and Department of Physics, University of Colorado, Boulder, Colorado 80309, USA

(Received 3 March 2004; revised manuscript received 30 November 2004; published 22 June 2005)

This paper demonstrates that transverse beam halos can be controlled by combining nonlinear focusing and collimation. The study relies on one-dimensional, constant focusing particle-in-cell (PIC) simulations and a particle-core model. Beams with linear and nonlinear focusing are studied. Calculations with linear focusing confirm previous findings that the extent and density of the halo depend strongly upon the initial mismatch of the beam. Calculations with nonlinear focusing are used to study damping in the beam oscillations caused by the mismatch. Although the nonlinear force damps the beam oscillations, it is accompanied by emittance growth. This process is very rapid and happens within the first 2–3 envelope oscillations. After this, when the halo is collimated using a system of four collimators, further evolution of the beam shows that the halo is not regenerated. The elimination of the beam halo could allow either a smaller physical aperture for the transport system or it could allow a beam of higher current in a system with the same physical aperture. This advantage compensates for the loss of particles due to collimation.

DOI: 10.1103/PhysRevSTAB.8.064202 PACS numbers: 29.17.+w, 29.27.Bd, 41.75.−i

I. INTRODUCTION

A major issue facing the functioning of high current accelerators is beam halo formation. High current accelerators find applications in heavy ion fusion, nuclear waste treatment, production of tritium, production of radio isotopes for medical use, and spallation neutron sources [1]. The halo is formed by a small intensity distribution of particles surrounding the core of the beam. When such particles drift far away from the characteristic width of the beam, their loss will lead to the production of residual radioactivity of the accelerating system. Many of the above applications require that the number of particles lost to the system must be less that one part in 10^5–10^6. With such a stringent requirement, methods to control the beam halo can prove very useful. However, there has been relatively less effort spent on devising such methods when compared to the extensive study that has already been done to understand the physics of beam halo formation. The methods employed to study beam halos include analytic models, multiparticle simulations using mainly the particle-core model and PIC simulations [2–21], and also experimental studies [22,23].

The dependence of the extent of beam halos and the initial beam mismatch has been studied by Wangler *et al.* [15], where it is shown that the maximum dimensionless particle amplitude $X_{\max}$, which is the distance with respect to the matched beam width, can be described by an approximate empirical formula, which is,

$$X_{\max} = A + B|\ln(\mu)|. \tag{1}$$

Here, A and B are weak functions of the tune depression ratio approximately given by $A = B = 4$ [15], and μ is the initial beam mismatch ratio. This result is not a good estimation of maximum amplitude for μ close to 1. It has also been shown [24] that in addition to increased halo extent, the number of halo particles grows with increased initial mismatch ratio. Batygin [25] showed that one can obtain a better match through nonlinear focusing for a prescribed charge distribution leading to reduced halo. Thus, it is already well established that reducing the beam mismatch can be an important factor in halo mitigation.

O'Connell *et al.* [3] traced the trajectories of various test particles with different initial conditions for a beam in a constant, linear focusing channel. This led to the discovery of ''hybrid'' trajectories, which undergo a resonant interaction with the core which was later analyzed by Gluckstern [2]. The discovery of these hybrid trajectories reveals the limitations on the effectiveness of a one time beam collimation because the continued resonant interaction causes the halo to almost always regenerate [2]. This issue will be addressed in this paper. The removal of halo in periodic linear focusing systems has been studied previously [24] where a series of 14 collimators were used.

In the present paper, we propose reducing mismatch by damping the transverse oscillations of the beam through nonlinear focusing before collimation to avoid the need for repeated collimation. Collimation still becomes essential in this process due the emittance growth accompanying the nonlinear damping. Our studies are based on a radial particle-in-cell (PIC) code along with some preliminary studies using a modified particle-core model. This paper is organized as follows. Section II describes a modified particle-core model for nonlinear focusing and examines the effect of nonlinear focusing on beams through this model. In Sec. III, the PIC algorithm and the physical model used to represent the beam has been described and simulation results of beam halo formation with different initial mismatches have been presented. In addition, results showing damping and emittance growth due to nonlinear focusing are also presented. The PIC simulation results are

then compared with the particle-core model results. Finally, Sec. IV shows results of a combination of nonlinear focusing and collimation.

II. RESULTS FROM A PARTICLE-CORE MODEL

The particle-core model in this paper serves the purpose of obtaining a qualitatively similar result with a simpler model, thus exhibiting the general nature of the phenomena of damping and emittance growth due to nonlinear focusing. For a linear focusing system, the core is generally represented by the envelope equation, which is not valid for a nonlinear focusing system. Since nonlinear focusing is used in this study, the core is simulated using a different method.

The envelope equation will still be used as a reference to determine parameters such as mismatch ratio and tune depression ratio. Consider a uniform, round, thin beam moving in the axial direction and with a constant axial velocity in a linear and constant focusing channel. Under these conditions, the envelope equation describes the oscillation of R, the radius of the beam with respect to the axial distance s which is a timelike variable for a beam with constant axial velocity. This can be expressed as (see, for example, [26,27])

$$\frac{d^2R}{ds^2} + k_0R - \frac{\epsilon^2}{R^3} - \frac{K}{R} = 0. \tag{2}$$

The focusing force is represented by k_0, K is the space charge perveance which depends upon the intensity, axial velocity, and charge to mass ratio of the particles [26,27]. The rms emittance of the beam ϵ is given by

$$\epsilon = 4\sqrt{\langle x\rangle^2\langle v_x\rangle^2 - \langle xv_x\rangle^2}, \tag{3}$$

where the angle bracket represents an average over the particle distribution in position space, x is displacement along the horizontal axis, and $v_x = dx/ds$. For a matched beam, the radius remains constant at $R = R_0$ satisfying the condition, $d^2R/ds^2 = 0$. It was shown by Sacherer [28] that the envelope equation can be generalized to even nonuniform distributions having elliptic symmetry (in this case, azimuthal symmetry). In such a case, the radius may be generalized to $R = 2a$ and $R_0 = 2a_0$, where a is the rms width of the beam, and a_0 is the matched rms width. We define a dimensionless displacement by $X = x/a_0$, a dimensionless velocity by $V_x = v_x/\sqrt{k_o}a_0$, a dimensionless axial distance given by $S = \sqrt{k_0}s$ and a dimensionless rms width given by $M = a/a_0$. The initial mismatch ratio, which is the initial value of M is represented as μ. All calculations will be made with respect to these dimensionless quantities.

The tune depression ratio, $\eta = \epsilon/\sqrt{k_0}R_0^2$ is a dimensionless quantity which gives a measure of the ratio between the wave numbers (or equivalently, frequencies) of a particle oscillating with and without the effect of space charge, respectively. While this ratio is exact for any in-core particle in a uniform distribution core, the definition may be extended to provide information on a general beam, especially to determine if a beam is space charge dominated or emittance dominated. A tune depression ratio close to unity represents an emittance dominated beam while if η is much less than unity, it is a space charge dominated beam.

In this paper, the core was simulated through a series of 600 infinitely long charged cylindrical "sheets" which could move radially inward or outward. The field on test particles and the sheets of the core were calculated from Gauss's law using a flux weighted averaging scheme [29]. The test particles did not contribute to the field. The sheets representing the core were advanced in the radial direction while the test particles were moved along the "x" and "y" coordinates. In both the cases, the leap frog scheme was used.

The sheets representing the core, and the test particles, in units of mass $m = 1$, satisfy the following equation,

$$\frac{d^2r}{ds^2} = F + F_{sc} + \frac{L^2}{r^3}, \tag{4}$$

where r is the radial distance and s is still the distance along the axis, F is the focusing force, F_{sc} is the space charge force, and L is the angular momentum which is set to zero for the sheets. The purely linear focusing force had the form

$$F = -k_0r, \tag{5}$$

while the focusing force with the nonlinearity included had the form

$$F = -k_1r - k_2r^3. \tag{6}$$

The corresponding space charge densities that balance the focusing force will be equal to

$$\rho = 2\frac{\epsilon_0}{e}k_0 \tag{7}$$

and

$$\rho = \frac{\epsilon_0}{e}(2k_1 + 4k_2r^2), \tag{8}$$

respectively, for $r < R_0$, and equal to zero for $r > R_0$, where R_0 is the radius of the matched beam. Here, e is the charge on the particle and ϵ_0 is the permittivity in free space. A mismatch is introduced by expanding or contracting the core and uniformly scaling the charge density to ensure conservation of charge. In performing the calculations in this section, we used a core which was expanded to 1.35 times its matched width. All the sheets comprising the core were initially at rest. In the absence of a nonlinearity, the density of the core is uniform, corresponding to a Kapchinskij-Vladmirskij (KV) distribution [30].

Based on the parameter a_0, the matched rms width according to the envelope equation, we set the linear and

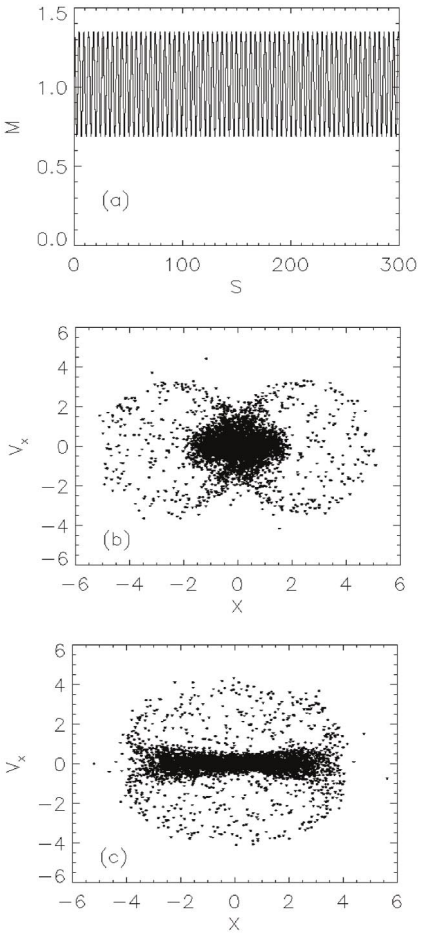

FIG. 1. Linear oscillations. (a) Oscillation of the rms width of the core with $\mu = 1.35$, (b) test particle distribution at last minimum rms width when $S \leq 300$, (c) test distribution at last maximum rms width when $S \leq 300$.

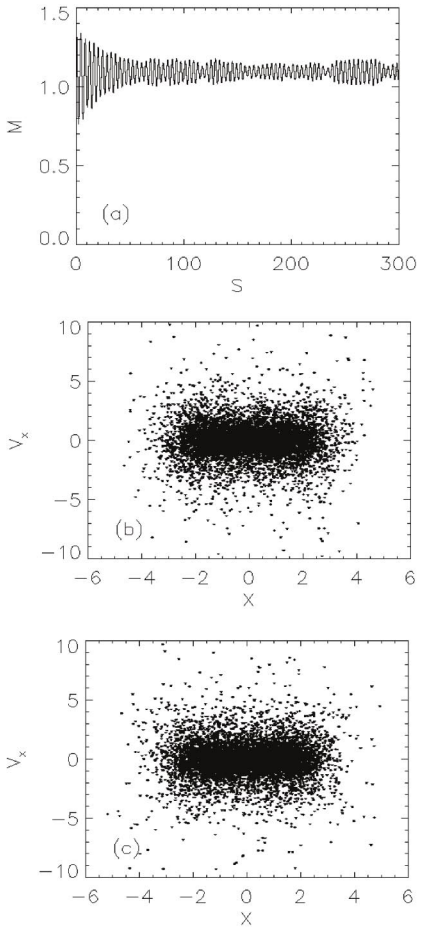

FIG. 2. Nonlinear oscillations. (a) Oscillation of the rms width of the core with $\mu = 1.35$, (b) particle distribution at last minimum rms width when $S \leq 300$, (c) distribution at last maximum rms width when $S \leq 300$.

nonlinear focusing parameters such that they satisfied the conditions

$$k_0 a_0 = k_1 a_0 + k_2 a_0^3 \tag{9}$$

and

$$\frac{k_1}{k_2 a_0^2} = 4. \tag{10}$$

Equation (9) indicates that the linear and nonlinear focusing forces were equal at the characteristic distance a_0, and Eqs. (9) and (10) together give a measure of how much the linear force was reduced before introducing the nonlinear component. To study the distribution of the particles, 10 000 test particles were used which had an initial Gaussian distribution in four dimensional phase space with an rms width equal to half the initial radius of the core. In the linear case, this makes the core and particle distribution equivalent according to the envelope equation. The initial distribution was identical for the linear and nonlinear case corresponding to a tune depression of 0.1 in the linear focusing channel. The initial mismatch of the test particle distribution as predicted by the envelope equation for the linear focusing case was 1.35, identical to that of the core.

Figure 1(a) shows about 70 oscillations of the rms width of the core. These oscillations are sustained in the linear focusing case because all the sheets in the core are oscillating in phase and at the same frequency. The corresponding phase space distribution of the test particles that are moving under the influence of the core are plotted when the rms width of the core is at its minimum and its maximum, respectively. Over here, we choose the last minimum and maximum point that appears in Fig. 1(a), i.e., when $S \leq 300$. Figure 1(b) shows the phase space distribution at this minimum rms width, while in Fig. 1(c), the distribution is at the corresponding maximum rms width.

When nonlinearity is introduced, not only does the density become nonuniform, but the frequency distribution of the oscillations of the charged sheets for a mismatched beam also becomes nonuniform. This is expected to lead to damping of the oscillation in the rms width of the core as seen in Fig. 2(a). The mechanism is well known in many

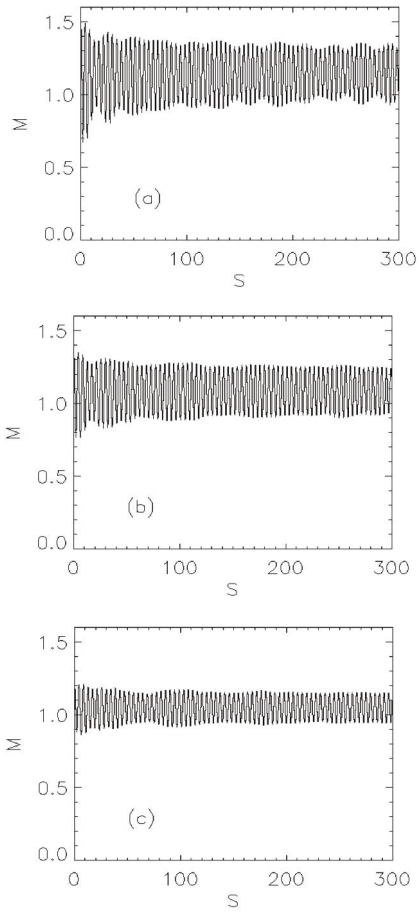

FIG. 3. Oscillation of the rms width of the beam for $\mu =$ (a) 1.5, (b) 1.35, (c) 1.2.

branches of physics as Landau damping. In the damping process, the velocity spread of the beam increases (the beam is heated). Figure 2(b) shows the corresponding phase space distribution of test particles moving under the influence of this core (a) when the rms core width was at the last minimum seen in Fig. 2(a), and in Fig. 2(c), the core was at the last maximum rms width when $S \leq 300$.

It is easily noticed that the width of the core does not change significantly due to the damping of the oscillations. This would simplify the task of collimating the halo. Since the collimator radius has to be larger than the radius of the core, the phase of the core oscillation becomes an important factor in the linear focusing case, where the core is seen to expand up to twice its minimum size. Figures 2(b) and 2(c) also show that the beam spreads out in velocity space, while the spread in position space is comparable to the linear focusing case. The spread in velocity is due to a transfer of energy from the mismatched core to the velocity distribution of the particles. However, due to the nonlinear focusing, the particles having a higher kinetic energy must also overcome a stronger potential gradient as they drift away from the core. This restricts the spread in position space, which helps restrict the radius of the collimator.

III. RESULTS FROM PIC SIMULATIONS

The evolution of the beam is now simulated using a radial PIC code. In these calculations, the charge distributions and forces used were azimuthally symmetric, a simplified model for which a one-dimensional field solver is sufficient. Since the fields vary along the radial direction, they are solved using Gauss's law over a radial grid. The particles, however, are advanced using the leap frog scheme in Cartesian coordinates along the x and y axis. This helps avoid problems arising due to singularities at the origin if radial and azimuthal motion was used [31]. The particles are distributed over the grid using area weighting while the fields were assigned to the particles using flux weighted averaging [29].

We examine the halo generated for beams with different initial mismatch ratios. The beam had an initial Gaussian distribution in four dimensional phase space. The tune depression calculated from the corresponding envelope equation was chosen to be 0.1 for all the cases, which implies that the beam was space charge dominated. We used 100 000 particles in all the PIC simulations, which was large enough for the particle distributions to retain the

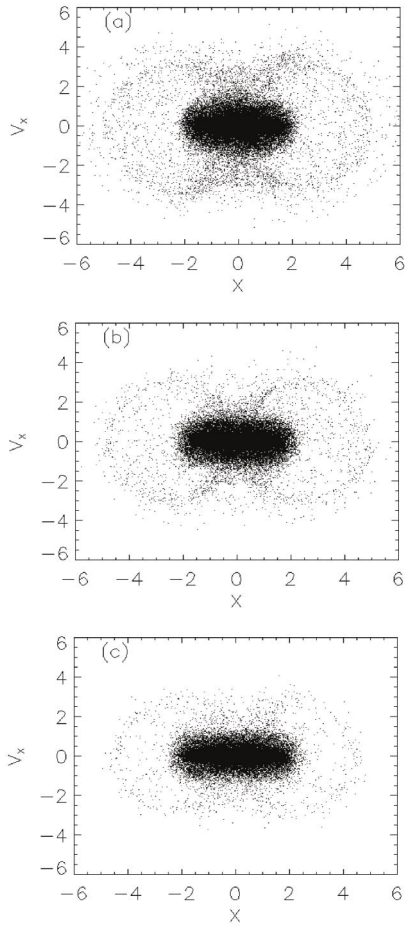

FIG. 4. Phase space distribution at last minimum rms width when $S \leq 300$ for $\mu =$ (a) 1.5, (b) 1.35, (c) 1.2.

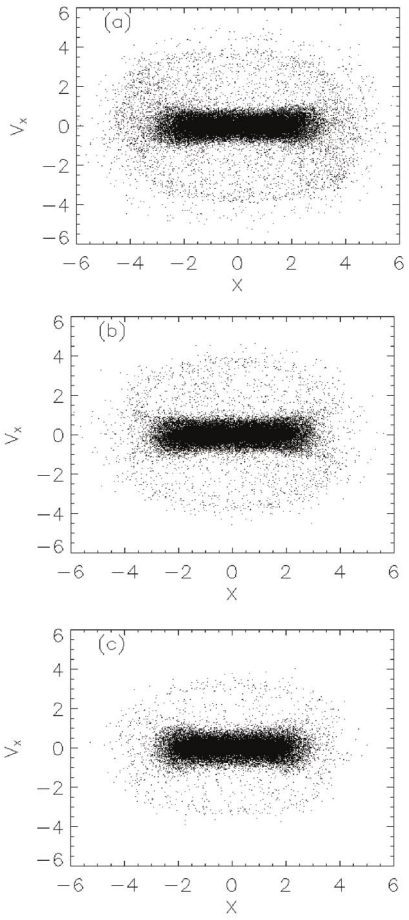

FIG. 5. Phase space distribution at last maximum rms width when $S \leq 300$ for $\mu =$ (a) 1.5, (b) 1.35, (c) 1.2.

desired azimuthal symmetry. These particles were distributed over 500 radial cells distributed over a length $10a_0$.

Figure 3 shows about 70 oscillations of the normalized rms width of the beam with an rms mismatch ratio μ of (a) 1.5, (b) 1.35, and (c) 1.2. It may be noticed that there is some initial damping of the oscillations after which a steady pattern emerges. The small initial damping could be attributed to the fact that a Gaussian distribution does not correspond to a Vlasov-Poisson equilibrium, so in the initial stage of the beam oscillation, one could expect some remixing of the distribution in phase space.

To examine the halo formation in these beams, the phase space distribution of the particles is then taken toward the end of the oscillations for two cases, which are (i) when the rms width of the distribution is a minimum, shown in Fig. 4 and (ii) when it is a maximum, shown in Fig. 5. The minimum and maximum points were the last ones seen in Fig. 3, that is, when $S \leq 300$. The relative change between the maximum and minimum width of the core agrees very well with that obtained using the particle-core model for the corresponding initial mismatch of 1.35. It can also be seen that the extent and intensity of the halo increases with increased mismatch, which confirms the need to obtain a reduced mismatch in order to control halo formation.

Figure 6 shows about 90 rms oscillations along with initial damping caused by the nonlinear focusing. The nonlinear focusing is of the same form as Eq. (6) satisfying the condition given by Eqs. (9) and (10), where a_0 is the matched rms width of the beam. The initial distributions were identical to the ones used in the linear focusing case. The parameter μ when defined for a nonlinear focusing case corresponds to the mismatch ratio in the linear focusing channel for the same initial distribution. It may be noticed that the damping takes place in the first 1–2 rms oscillations while it takes about 5–6 oscillations in the particle-core model. Also, the final amplitude of the oscillation after the damping is seen to decrease with a decrease in μ, the initial ''mismatch.''

Figures 7 and 8 show the corresponding phase space distributions of the particles when the rms width was a minimum and a maximum, respectively. Once again, the minimum and maximum points are the last ones seen in Fig. 6 for the corresponding mismatch. The observations show good agreement with the particle-core model results. That is, the rms width of the beam does not change

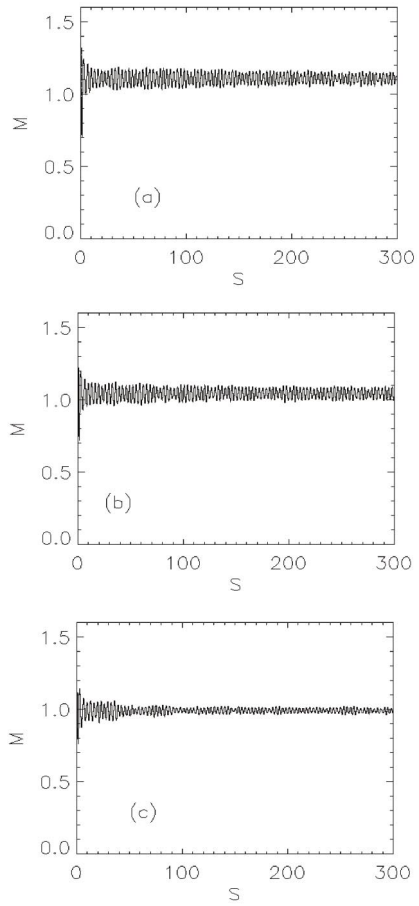

FIG. 6. Oscillation of the rms width of the beam with nonlinear focusing for $\mu =$ (a) 1.5, (b) 1.35, (c) 1.2.

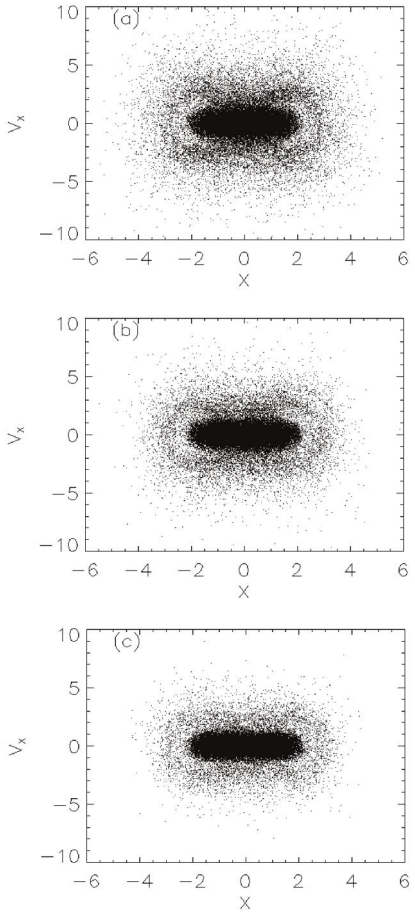

FIG. 7. Oscillation of the rms width of the beam with nonlinear focusing at the last minimum rms width when $S \leq 300$ for $\mu =$ (a) 1.5, (b) 1.35, (c) 1.2.

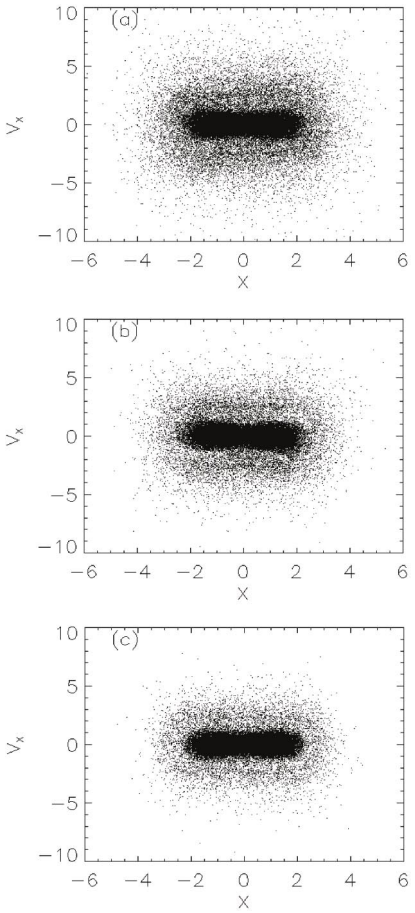

FIG. 8. Oscillation of the rms width of the beam with nonlinear focusing at last maximum rms width when $S \leq 300$ for $\mu =$ (a) 1.5, (b) 1.35, (c) 1.2.

significantly, as a consequence of the damping, and the particles spread far in velocity space while their spread in position space is comparable to the linear focusing case.

Despite the fact that the space charge force in the particle-core model is created by an oscillating core, while in the PIC simulations, the particles are influenced by a self-consistent space charge force, both the models in general show a remarkably similar response to nonlinear focusing. However, we see in Fig. 6 that the damping is more rapid in the PIC simulations. For the same initial conditions used in both the models, which is $\mu = 1.35$, the size of the core and the extent of the halo was the same for both linear and nonlinear focusing.

IV. COLLIMATION WITH NONLINEAR FOCUSING

This section will show that the combination of nonlinear focusing and collimation eliminates the beam halos permanently. For the sake of consistency, the rms width of the beam was at a maximum when collimation was started for all the cases. However, it has been shown previously in this paper that the phase of the oscillation is not a critical factor due to the nonlinear damping, so collimation could have been performed at another phase of rms oscillation to get similar results.

In this case, we used a series of four collimators that were separated by a dimensionless axial distance of $S = 0.75$. Thus the total length of the collimation section is $S = 2.25$. This is less than one period of the rms oscillation which had an approximate value, $S = 3.3$. This separation between adjacent collimators, which is a small fraction of an rms oscillation, is possible because the halo particles, which have high amplitudes are also oscillating at a greater frequency due to the nonlinear component in the focusing. Since the size of the core does not change significantly between maximum and minimum as shown in the previous section, the adjacent collimators can be placed close enough without the concern that the core radius would exceed the collimator radius. The point of collimation was always chosen to be the first maximum rms width after a period of $S = 50$ which corresponds to about 15 rms oscillations.

There is no established quantitative definition as yet of a beam halo although recent efforts are being made to quan-

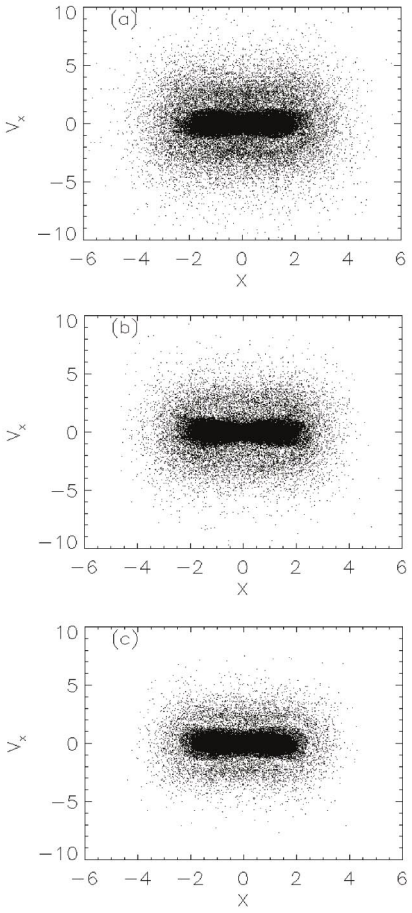

FIG. 9. Phase space distribution of particles just before collimation for a beam with nonlinear focusing for $\mu =$ (a) 1.5, (b) 1.35, (c) 1.2.

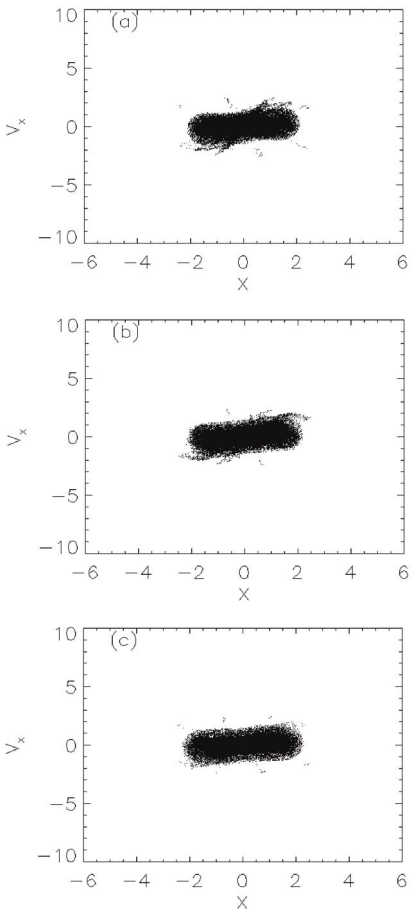

FIG. 10. Phase space distribution of particles just after collimation for a beam with nonlinear focusing for $\mu =$ (a) 1.5, (b) 1.35, (c) 1.2.

tify such a halo [32]. This leads to some uncertainty in the optimum choice of the collimator radius. In this study, the edge of each of these four collimators satisfied the equation

$$X^2 + Y^2 = c^2. \tag{11}$$

The value c was chosen as 2.5 which was based on an assumed requirement that the final maximum extent of the beam did not exceed the dimensionless radial distance of 3.0 for any the three mismatch values. This is roughly half the maximum extent of the beam for the highest mismatch of $\mu = 1.5$ used in our study and in the absence of collimation. A slightly larger collimator radius produced a distribution that exceeded this limit. Table I in this section shows that the number of particles lost due to collimation decreases with reduced mismatch for the same collimator system. Thus, having a small initial mismatch is still an advantage but this is not possible to achieve in most practical applications.

Figure 9 shows the distribution of the particles just before collimation. The distribution of these particles is very similar to that seen in Fig. 8 although they were taken at a much earlier stage, i.e., after about 15 rms oscillations as opposed to about 90. This shows that there is little change as the beam propagates once the damping has been achieved.

Figure 10 shows the distribution just after collimation. It is noticeable that the velocity distribution has been efficiently scraped off with the set of four collimators together lying well within one rms oscillation period. As mentioned previously in this section, this is a consequence of the increase in frequency of oscillation of the particles with an increase in amplitude which would not occur with purely linear focusing.

Figure 11 shows the oscillation of the beam along with the collimation. The rms size of the beam abruptly drops due to the elimination of particles far away from the center. It may be noticed that the damping is not affected and is sustained even after the collimation is performed which is an important phenomenon that ensures that the halo is not reproduced, i.e., the advantages of reduced mismatch are retained.

Figure 12 shows the distribution of particles at the point of the last maximum rms width seen in Fig. 11. It is clear that the particles that stray far away from the core are

TABLE I. The mismatch and corresponding particle loss due to collimation.

$\mu = 1.5$	Particle loss = 19.1%
$\mu = 1.3$	Particle loss = 13.7%
$\mu = 1.2$	Particle loss = 8.2%

completely eliminated. These figures may be compared with the corresponding ones in the previous section for the same mismatch with linear focusing. Although the distributions were taken when the rms width was a maximum, this would not make a significant difference from another phase of the rms oscillation since their amplitudes are already well damped. The extent of the beam remains the same after this process regardless of the initial mismatch, while, the number of particles lost in the collimation increases with increased mismatch.

The large spread in velocity space, which is a result of the nonlinear damping implies that more particles need to be collimated away. Despite this drawback, the absence of a halo would enable one to have a broader beam that would more than compensate for the additional loss in particles. For example, assume that particles cannot be allowed beyond a distance of $X = 3$. The particle distributions shown in Fig. 12 clearly satisfy the restrictions, while the ones shown in Figs. 4 and 5 do not because of the extended halo produced due to linear focusing. In addition to this, the core itself stretches to $X = 3$ for linear focusing as seen in Fig. 5 while Fig. 12 shows that even the at maximum rms width, the beam is restricted to well within a distance of $X = 3$. All this implies that the initial beam will have to be considerably narrower in the case of linear focusing in order to restrict the halo to within a distance of $X = 3$ and thus allowing fewer particles in the channel. Another point to be noted is that the nonlinear focusing allows a more efficient collimation process. The large frequency of oscillation of the halo particles enables the collimators to be placed close to each other which also helps to reduce the number of collimators required, while the damped rms oscillations ensures that the positioning of the collimator does not depend upon the phase of the rms oscillation of the beam in order to avoid scraping into the ''core.'' These factors help achieve the required collimation in less that

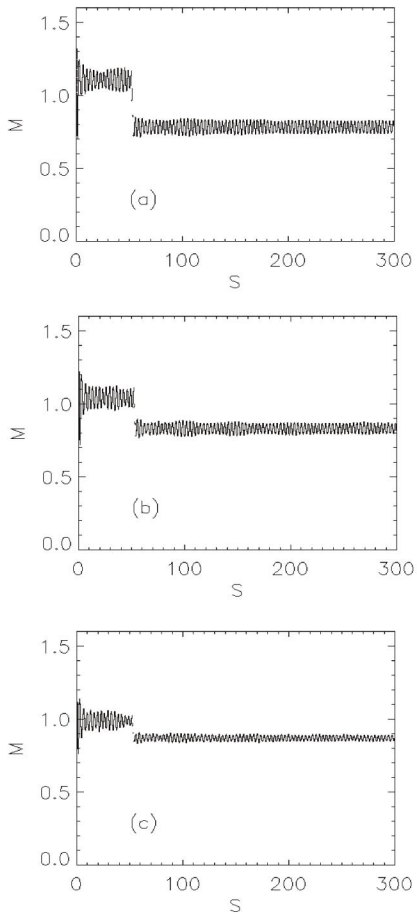

FIG. 11. Oscillation of the rms width of the beam with nonlinear focusing showing collimation for $\mu =$ (a) 1.5, (b) 1.35, (c) 1.2.

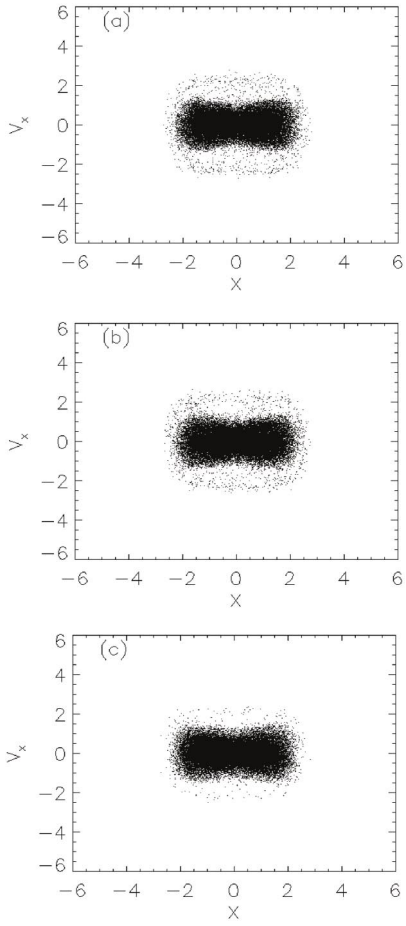

FIG. 12. Phase space distribution at the end of of oscillations shown in Fig. 11 at the last maximum rms width when $S \leq 300$ for $\mu =$ (a) 1.5, (b) 1.35, (c) 1.2.

one complete rms oscillation of the beam and with just four collimators.

V. SUMMARY

In this paper, we have proposed a new method that combines nonlinear damping and collimation to control beam halos. Our results showed that particles oscillating with large amplitudes compared with the width of the core can be completely eliminated with this mechanism making the need for repeated collimation unnecessary.

Particle-core and PIC simulations showed that nonlinear focusing leads to damping, thus reducing the beam mismatch. However, the damping was accompanied by the particle distribution spreading in the velocity space. This is a result of transfer of energy stored in the mismatch to the velocity distribution of the particles. The high velocity particles are prevented from straying far away from the beam due to the strong focusing force exerted by the nonlinear component at large radial distances. The beam was collimated using a four collimator system soon after the nonlinear damping was achieved, and the damped oscillations prevented further halo formation. Results showed that the particles with large amplitude oscillations were completely eliminated. A possible drawback of this process is the spread of particles in velocity space because of which the collimation process results in a loss of particles. However, we have argued that the knowledge that beam halos are controlled would enable one to extend the beam closer to the walls of the channel, thus increasing the beam current that would more than compensate for the loss in collimation.

It must be mentioned that the model used here was idealized in many respects because it had constant focusing and was purely radial. While this system is nearly integrable in the absence of space charge, this would not typically be true in real systems with nonlinear focusing components. This is because the Courant-Snyder invariants [33] are broken when nonlinear focusing components such as sextupoles or octupoles are used. This will cause the orbits to be chaotic leading to poor confinement even in the absence of space charges. However, it has been shown that [34] it is possible to reduce the nonlinear system to an equivalent, continuous, and radially focusing one upon averaging over the lattice period given that the nonlinear components are arranged in a specific manner along with an alternate gradient quadrupole focusing system. It has also been shown that this symmetry can be retained in the presence of space charge forces [35] and an equivalent equilibrium distribution exists for such a lattice. We propose the use of such a lattice for further study involving a two dimensional study.

Since the method proposed in this paper is not specific to a particular application, different applications will demand conditions that may be different from the ones used in this paper. For example, collimation of the halo is being studied for the Spallation Neutron Source accumulator ring [36]. The collimators use scrapers and absorbers to clean the transverse halo. The accumulator ring already has a straight section dedicated to the collimation system. Applying the proposed method proposed to such a system will require more extensive study. This is because the tune depression in this ring is close to unity, in contrast to the ones chosen in this paper. In addition to this, including nonlinear components in a ring will not be straightforward due to the effect of resonances and beam instabilities. However, one of the advantages of the proposed method is the fact that the nonlinear damping is only a transient process. Once the collimation is achieved, the system may be adiabatically matched to a linear focusing system. The possibility of such a matching has been analyzed by Batygin [37] and could be considered in such a study.

Less effort has been spent in devising methods to eliminate beam halos when compared to the extensive study of the properties of halo production itself. This paper could be an important step toward this direction. The results are encouraging enough to perform simulations in higher dimensions using nonlinear focusing components such as sextupoles or octupoles along with realistic designs for collimators.

ACKNOWLEDGMENTS

One of us (K. S.) wishes to thank Steve Lund and Alex Friedman for their input while writing the radial PIC code and to Yuri Batygin for some useful discussions. This work was supported by the U.S. Department of Energy under Grant No. DE-FG03-95ER40926. halomit

[1] D. Jeon *et al.*, Phys. Rev. ST Accel. Beams **5**, 094201 (2002).
[2] R. L. Gluckstern, Phys. Rev. Lett. **73**, 1247 (1994).
[3] J. S. O'Connell, T. Miller, R. S. Mills, and K. R. Crandall, in *Proceedings of the Particle Accelerator Conference, Washington, DC, 1993*, edited by S. T. Corneliussen (IEEE, Piscataway, NJ, 1993), p. 3757.
[4] J. Lagniel, Nucl. Instrum. Methods Phys. Res., Sect. A **345**, 405 (1994).
[5] J. Lagniel, Nucl. Instrum. Methods Phys. Res., Sect. A **345**, 46 (1994).
[6] R. A. Jameson, Los Alamos Report No. LA-UR-94-3753.
[7] T. P. Wangler, Los Alamos Report No. LA-UR-94-1135.
[8] C. Chen and R. A. Jemeson, Phys. Rev. E **52**, 3074 (1995).
[9] R. D. Ryan and S. Habib, Part. Accel. **55**, 365 (1996).
[10] H. Okamoto and M. Ikegami, Phys. Rev. E **55**, 4694 (1997).
[11] R. L. Gluckstern, A. V. Fedotov, S. S. Kurennoy, and R. D. Ryne, Phys. Rev. E **58**, 4977 (1998).
[12] A. V. Fedotov, R. L. Gluckstern, S. S. Kurennoy, and R. D. Ryne, Phys. Rev. ST Accel. Beams **2**, 014201 (1999).
[13] M. Ikegami, Phys. Rev. E **59**, 2330 (1999).
[14] T. Wang, Phys. Rev. E **61**, 855 (2000).

[15] T. Wangler, K. R. Crandall, R. Ryne, and T. S. Wang, Phys. Rev. ST Accel. Beams **1**, 084201 (1998).
[16] J. Qiang and R. Ryne, Phys. Rev. ST Accel. Beams **3**, 064201 (2000).
[17] R. L. Gluckstern, W.-H. Cheng, and H. Ye, Phys. Rev. Lett. **75**, 2835 (1995).
[18] R. L. Gluckstern, W.-H. Cheng, S. S. Kurennoy, and H. Ye, Phys. Rev. E **54**, 6788 (1996).
[19] S. Strasburg and R. C. Davidson, Phys. Rev. E **61**, 5753 (2000).
[20] N. C. Petroni, S. D. Martino, S. D. Siena, and F. Illuminati, Phys. Rev. ST Accel. Beams **6**, 034206 (2003).
[21] I. V. Sideris and C. L. Bohn, Phys. Rev. ST Accel. Beams **7**, 104202 (2004).
[22] C. K. Allen *et al.*, Phys. Rev. Lett. **89**, 214802 (2002).
[23] M. Reiser *et al.*, Phys. Rev. Lett. **61**, 2933 (1988).
[24] M. Ikegami and H. Okamoto, Jpn. J. Appl. Phys. **36**, 7028 (1997).
[25] Y K. Batygin, Phys. Rev. E **57**, 6020 (1998).
[26] R. C. Davidson and H. Qin, *Physics of Intense Charged Particle Beams in High Energy Accelerators* (World Scientific, Singapore, 2001).
[27] T. P. Wangler, *RF Linear Accelerators*, Beam Physics and Accelerator Technology (John Wiley, New York, 1998).
[28] F. J. Sacherer, IEEE Trans. Nucl. Sci. **18**, 1105 (1971).
[29] C. K. Birdsall and A. B. Langdon, *Plasma Physics via Computer Simulation*, Plasma Physics (Adam Hilger, London, 1991).
[30] I. Kapchinskij and V. Vladimirskij, in *Proceedings of the International Conference on High Energy Accelerators and Instrumentation* (CERN Scientific Information Services, Geneva, 1959), p. 274.
[31] A. Friedman and S. Lund (private communication).
[32] C. K. Allen and T. P. Wangler, Phys. Rev. ST Accel. Beams **5**, 124202 (2002).
[33] E. D. Courant and H. S. Snyder, Ann. Phys. (N.Y.) **3**, 1 (1958).
[34] K. G. Sonnad and J. R. Cary, Phys. Rev. E **69**, 056501 (2004).
[35] K. G. Sonnad and J. R. Cary (to be published).
[36] N. Catalan-Lasheras, Y. Y. Lee, H. Ludewig, N. Simons, and J. Wei, Phys. Rev. ST Accel. Beams **4**, 010101 (2001).
[37] Y. K. Batygin, Phys. Rev. E **54**, 5673 (1996).